



Supplement of

Imprints of climate forcings in global gridded temperature data

Jiří Mikšovský et al.

Correspondence to: Jiří Mikšovský (jiri.miksovsky@mff.cuni.cz)

The copyright of individual parts of the supplement might differ from the CC-BY 3.0 licence.

a) 1901-1955

	GHG	Solar	Volc.	SOI	NAOI	AMOI	PDOI	TPI
GHG		0.46	-0.42	-0.01	-0.04	0.63	-0.15	-0.01
Solar	0.46		-0.24	0.11	-0.02	0.24	0.02	0.01
Volc.	-0.40	-0.20		0.02	0.10	-0.28	0.10	-0.03
SOI	-0.02	0.10	0.04		-0.01	0.00	-0.30	0.01
NAOI	-0.04	-0.02	0.08	0.00		-0.15	-0.05	-0.09
AMOI	0.63	0.25	-0.36	-0.07	-0.15		-0.02	0.00
PDOI	-0.15	0.00	0.13	-0.31	-0.05	-0.02		-0.01
TPI	-0.01	0.01	-0.03	0.02	-0.09	0.00	-0.01	
VIF	2.17	1.31	1.24	1.14	1.04	1.78	1.18	1.01

b) 1956-2010

	GHG	Solar	Volc.	SOI	NAOI	AMOI	PDOI	TPI
GHG		-0.06	-0.14	-0.05	-0.09	0.39	0.10	0.10
Solar	-0.06		-0.07	-0.05	0.11	0.13	0.03	-0.06
Volc.	-0.12	-0.14		-0.26	0.11	-0.31	0.17	-0.02
SOI	-0.07	-0.03	-0.19		-0.01	0.00	-0.45	-0.06
NAOI	-0.09	0.10	0.08	0.00		-0.16	-0.02	0.02
AMOI	0.39	0.12	-0.31	-0.08	-0.16		0.05	0.01
PDOI	0.10	0.06	0.23	-0.48	-0.02	0.05		0.00
TPI	0.10	-0.05	0.01	-0.02	0.02	0.01	0.00	
VIF	1.22	1.07	1.23	1.32	1.05	1.35	1.35	1.01

Table S1. As Table 1, for the 1901-1955 (**a**) and 1956-2010 (**b**) periods.

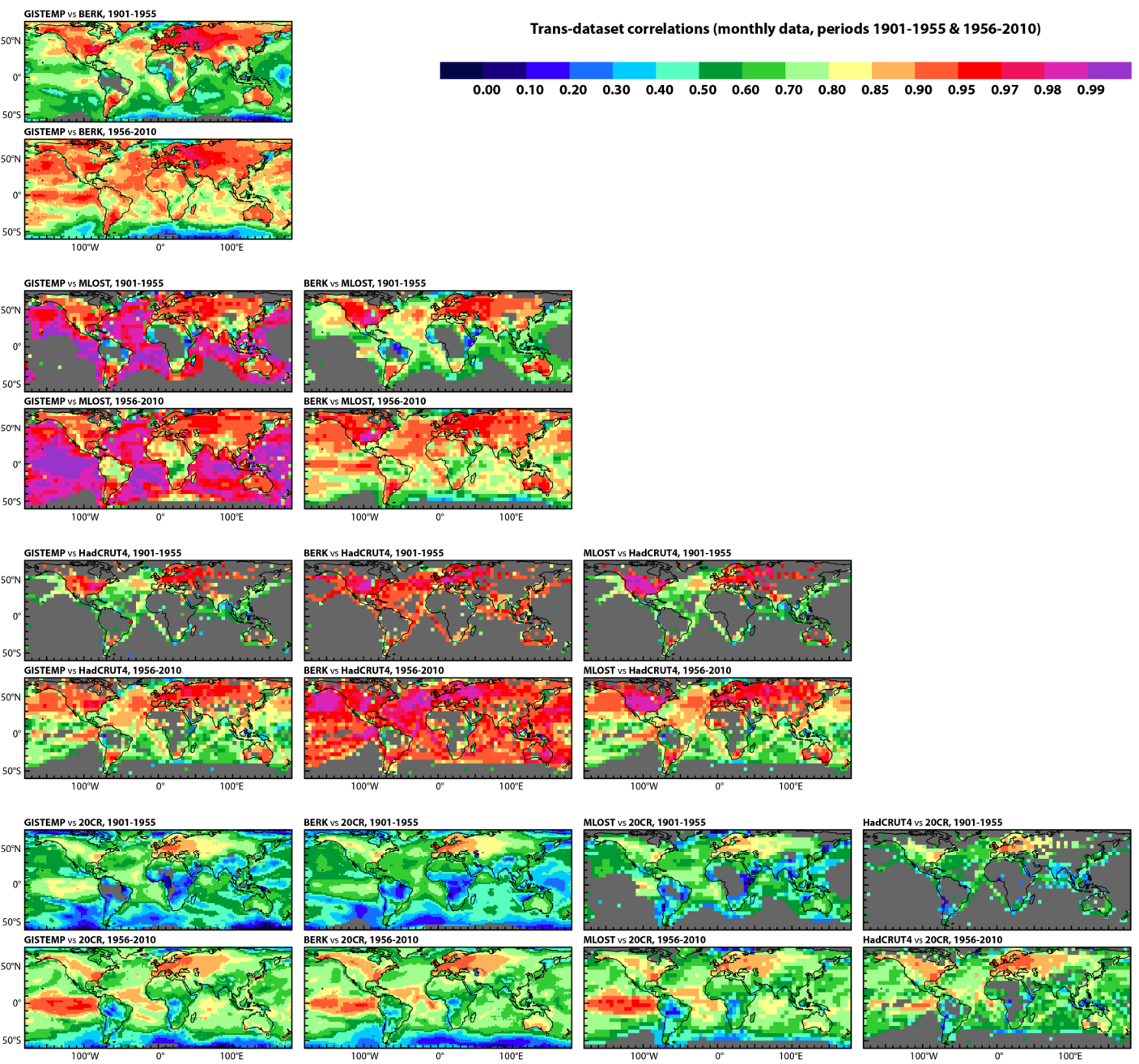


Figure S1. As Fig. 2, for sub-periods 1901-1955 and 1956-2010.

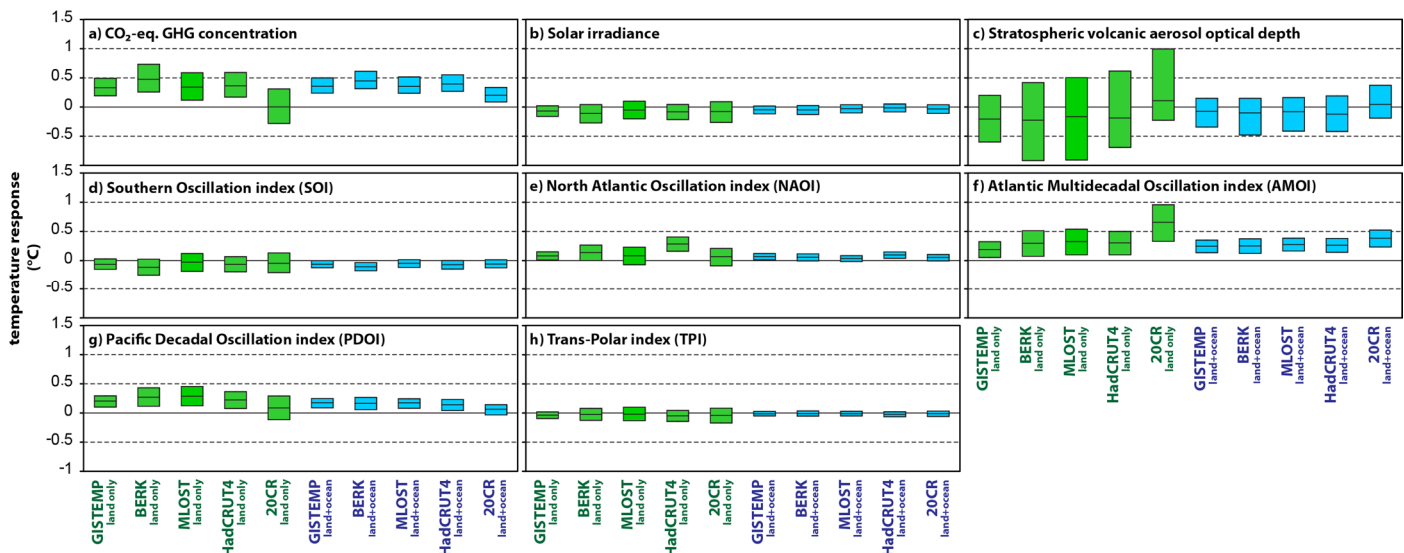


Figure S2. As Fig. 4, for the 1901-1955 sub-period. GHG-related response shown for CO₂-equivalent concentration increase between 1901 and 1955 (+29 ppm), volcanic response shown for Santa María-sized eruption (volcanic aerosol optical depth +0.08), the rest are shown for the predictor variations specified in Fig. 1.

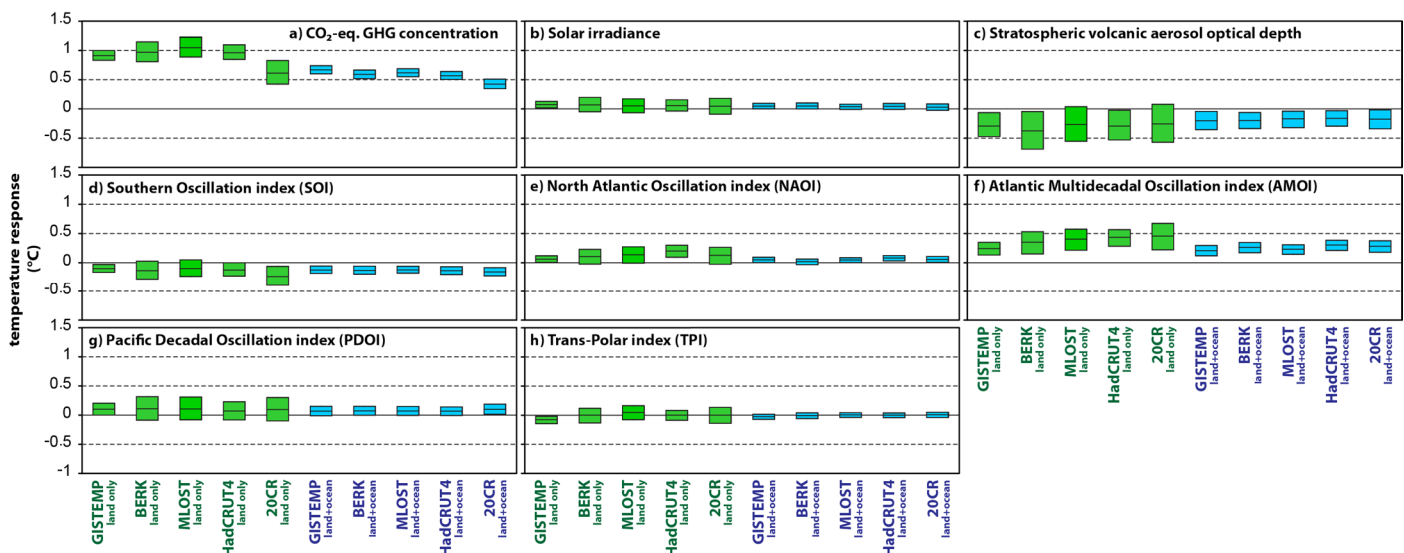


Figure S3. As Fig. 4, for the 1956-2010 sub-period. GHG-related response shown for CO₂-equivalent concentration increase between 1956 and 2010 (+112 ppm), the rest are shown for the predictor variations specified in Fig. 1.

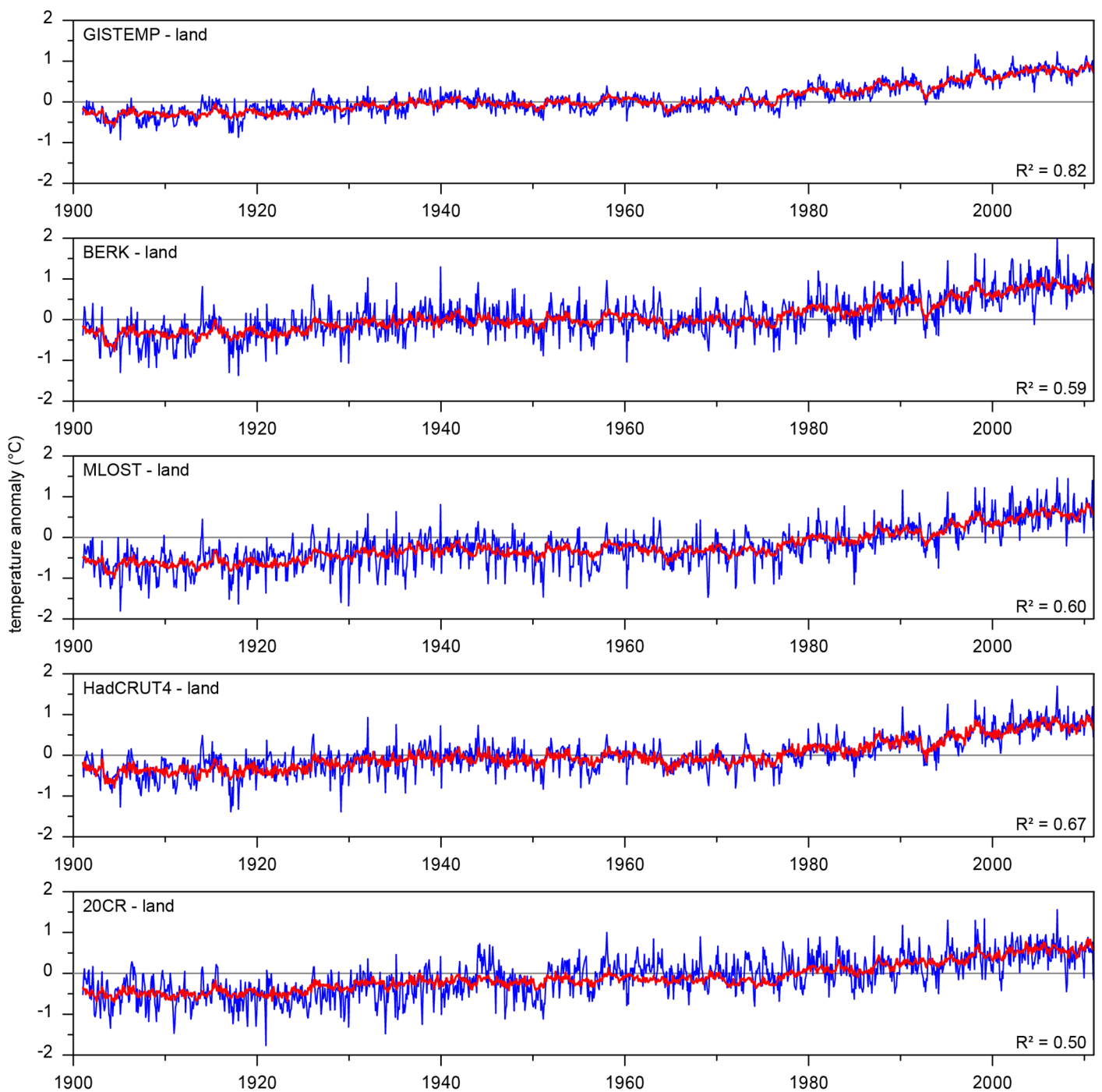


Figure S4. Series of globally averaged temperature, original (blue) and approximated by multiple linear regression (red). See Fig. 1 for visualization of the set of eight predictors entering the regression; Fig. 4 for the respective predictor-specific temperature responses.

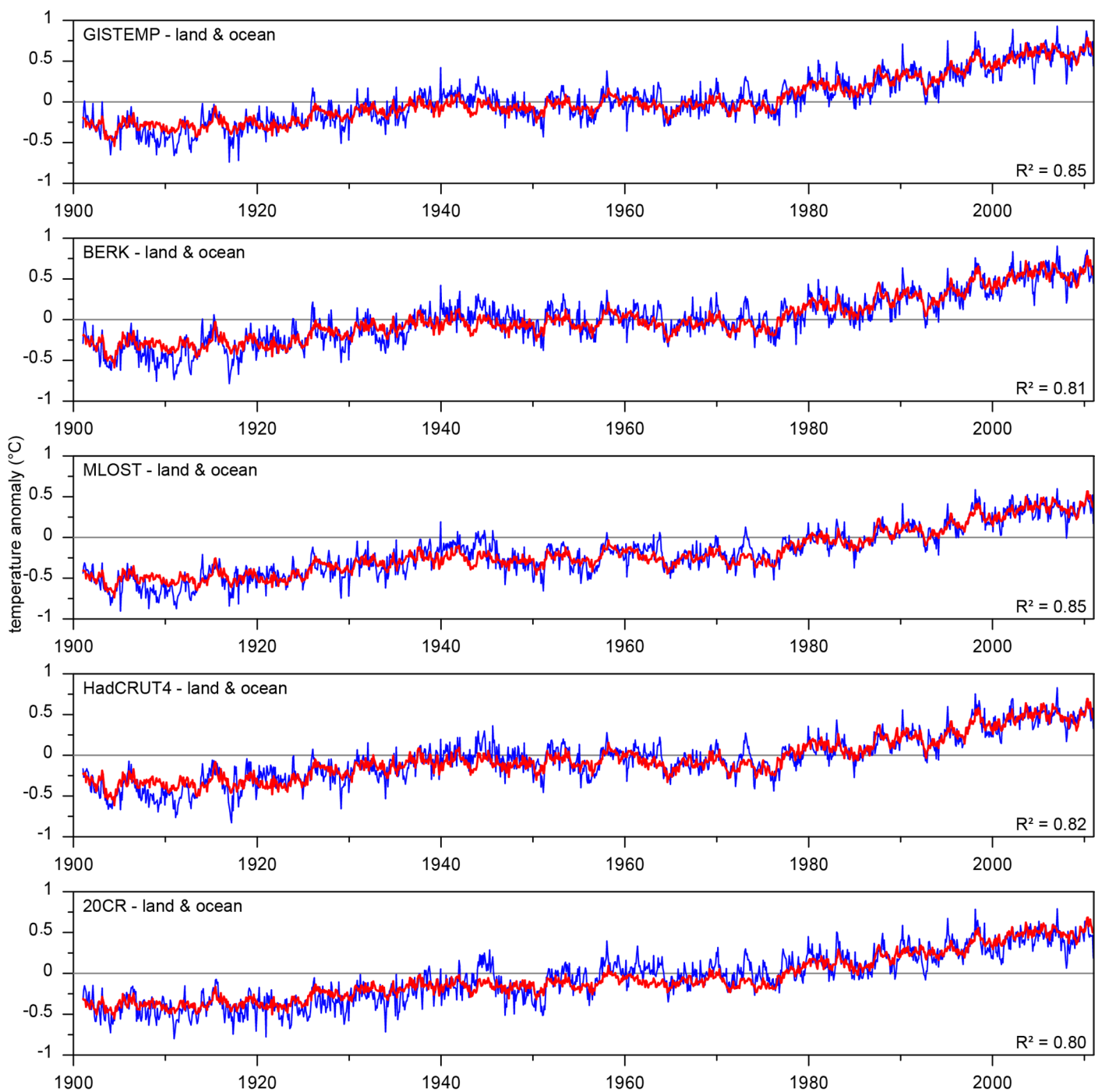


Figure S4. continued.

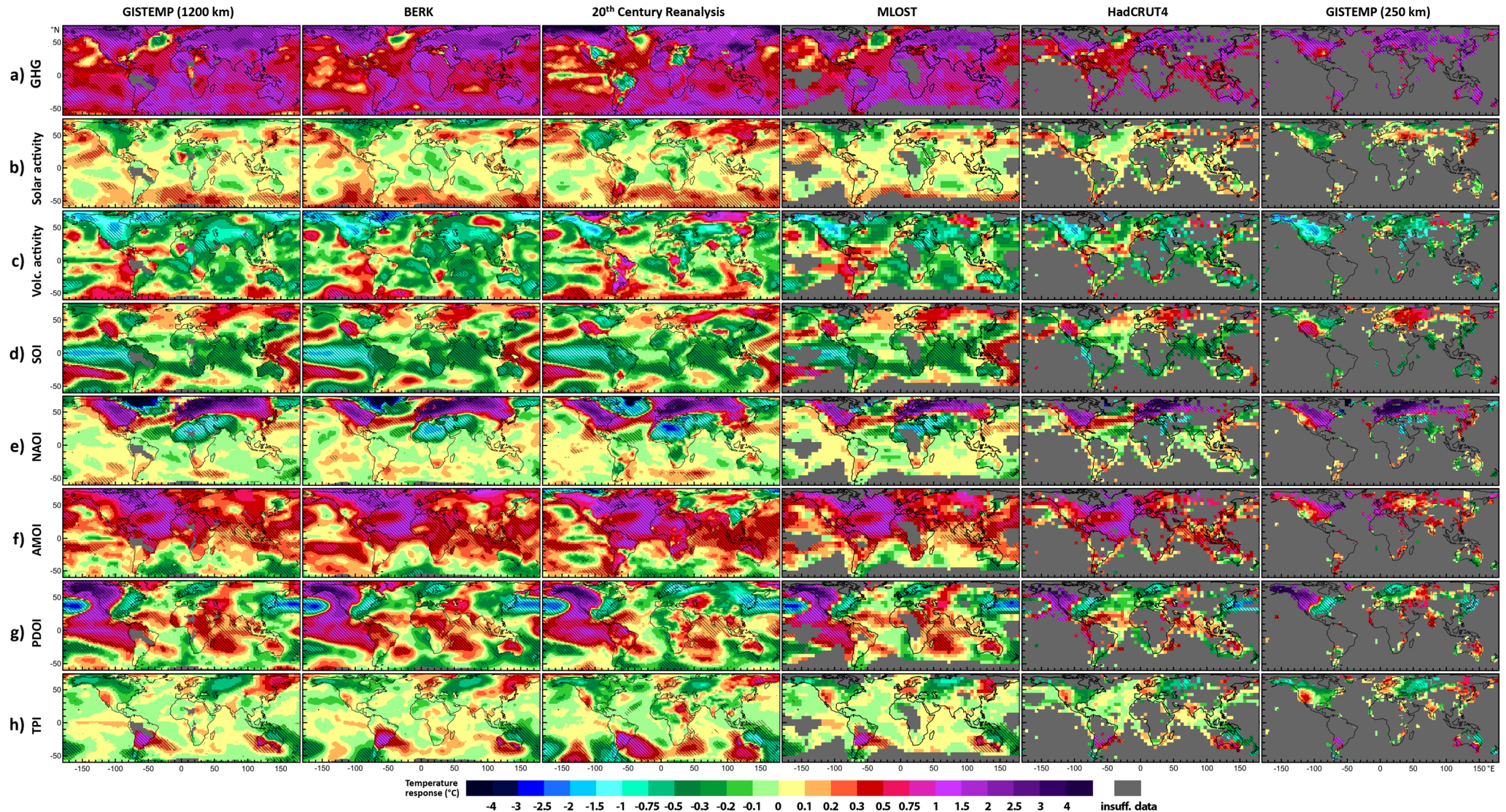


Figure S5. As Fig. 5, for all gridded temperature datasets. The results for GISTEMP are shown for both the version with 1200 km smoothing (i.e. the dataset investigated in the main text) and the version with 250 km smoothing.

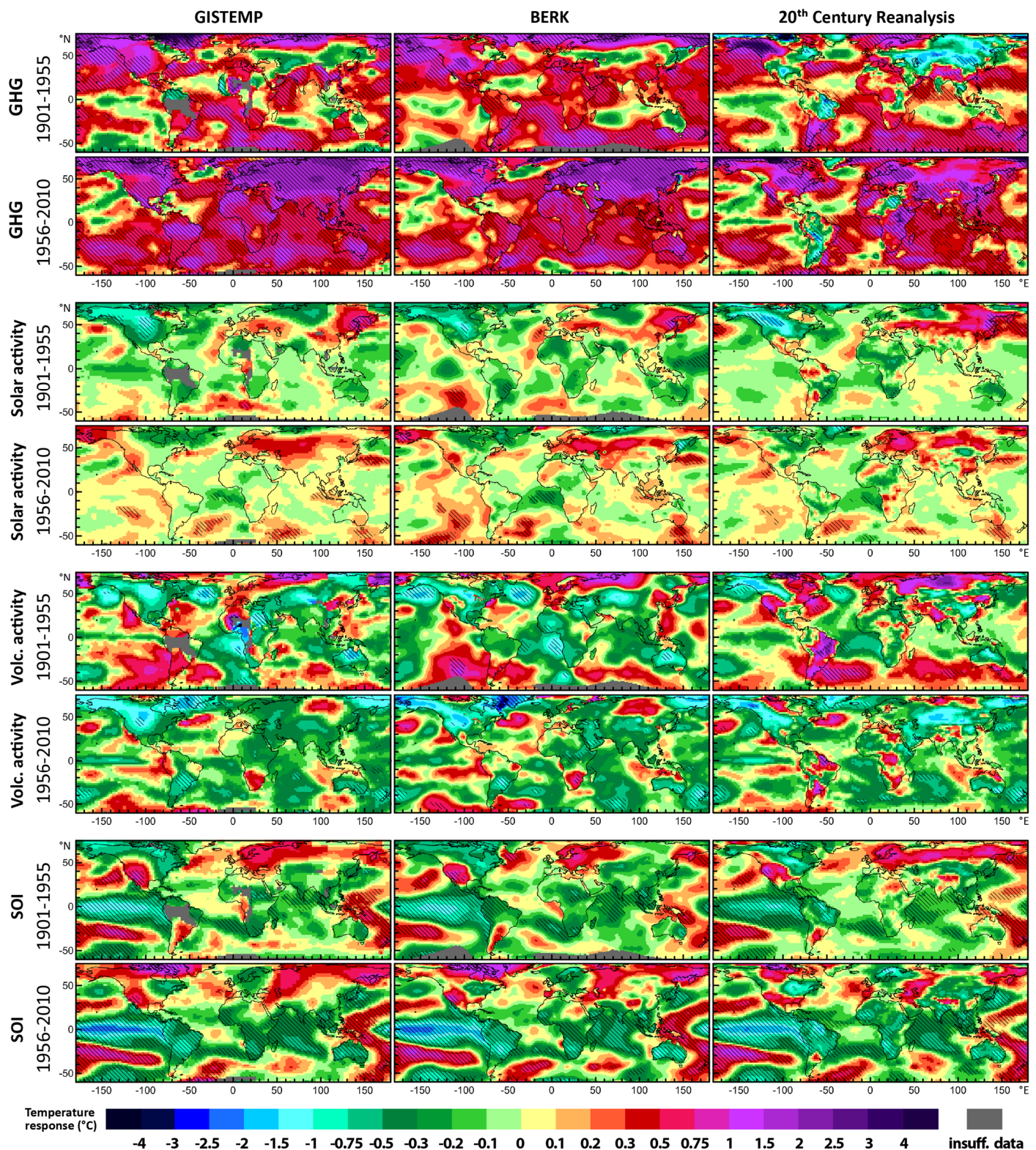


Figure S6. As Fig. 5, for sub-periods 1901-1955 and 1956-2010. GHG-related response shown for CO₂-equivalent concentration increase during the respective sub-periods (1901-1955: +29 ppm; 1956-2010: +112 ppm), volcanic-related response in 1901-1955 shown for Santa María-sized eruption (aerosol optical depth +0.08).

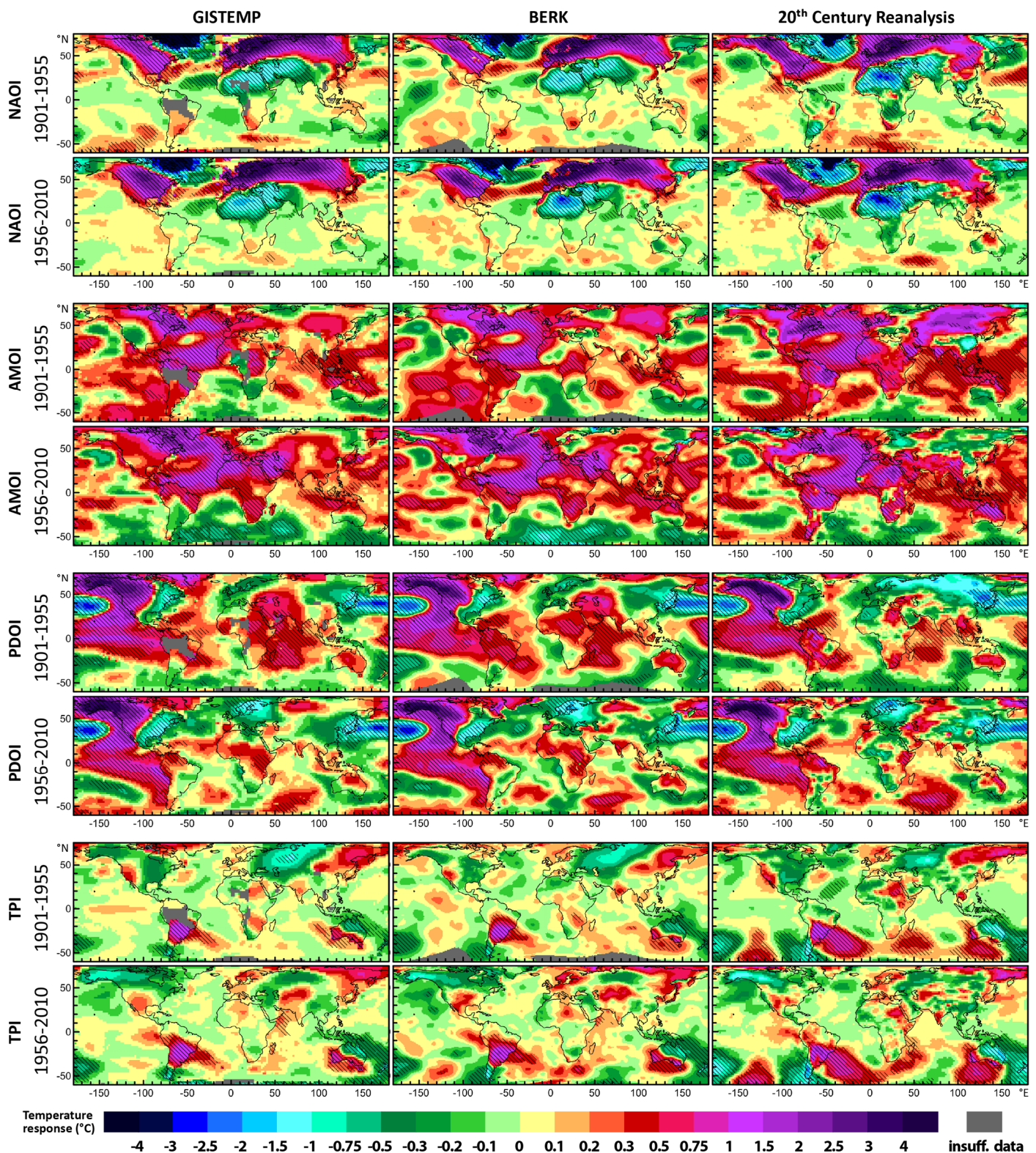


Figure S6. continued.